

Short Communication

## Effective Polysulfide Adsorption by Double Side Coated Separator in Lithium-Sulfur Batteries

Yulin Liu<sup>1</sup>, Jing Li<sup>1,2\*</sup>, Min Zeng<sup>1</sup>, Xun Xu<sup>1</sup>, Jianna Deng<sup>1</sup>, Jianqiang Guo<sup>1</sup>, Dan Zhao<sup>2</sup>, Jianzhao Yang<sup>3</sup>, Hongru Wang<sup>1</sup>,

<sup>1</sup> Institute of Material Science and Engineering, Southwest University of Science and Technology, Mianyang, 621010, Sichuan, China.

<sup>2</sup> Sichuan Xike Six Timbers Hi-tech Corporation, Mianyang 621010, China

<sup>3</sup> School of Environment and Resources, Southwest University of Science and Technology, Mianyang, 621010, Sichuan, China.

\*E-mail: [195216521@qq.com](mailto:195216521@qq.com)

Received: 17 March 2018 / Accepted: 6 May 2018 / Published: 5 July 2018

---

Lithium-sulfur batteries have attracted much attention because of their high specific capacity and energy density. However, the commercialization of lithium-sulfur batteries is limited by low utilization of active materials and excessive capacity decay which caused by the shuttle effect of polysulfide in the practical applications. In this article, effective polysulfide adsorption method was applied via using modified PP separator coated super P and Al<sub>2</sub>O<sub>3</sub> on the two sides, respectively. As a result, this strategy solves the problems of polysulfide shuttle effect and poor sulfur conduction at the same time. The initial discharge specific capacity of lithium-sulfur batteries, which assembled with the super P + PP + Al<sub>2</sub>O<sub>3</sub> separator, could reach 1247 mAh g<sup>-1</sup> at the current density of 0.1 C. After 60 discharge / charge cycles, the discharge capacity was still 987 mAh g<sup>-1</sup>, with a capacity retention of 79%. This method of simultaneous modification on both sides of the separator provides a new idea for the modification of lithium-sulfur batteries.

---

**Keywords:** super P layer, PP separator, Al<sub>2</sub>O<sub>3</sub> layer, shuttle effect, electrochemical performance

### 1. INTRODUCTION

With the rapid development of science and technology, the traditional lithium-ion battery capacity and energy density is difficult to upgrade. It can not satisfy the increasing needs for emerging electric bicycles, electric vehicles and mobile electronic devices in the future. Therefore, looking for high energy density storage system has become the urgent mission of scientists. Among these existing energy storage systems, lithium-sulfur (Li-S) batteries are considered as a new generation of energy

technology beyond lithium-ion batteries because of their high theoretical specific capacity and energy density [1-3]. More importantly, the raw materials (elemental sulfur) in the cathode are inexpensive and environmentally friendly.

Li-S batteries have indeed many advantages. However, the development of Li-S batteries is still restricted because of their poor cycling stability, which is mainly due to the low conductivity of elemental sulfur and the migration of soluble polysulfide in the process of charge / discharge named shuttle effect [4-7]. In order to solve these challenging problems in lithium-sulfur batteries, much attention has been paid to the structure design of cathode materials and electrolytes in Li-S battery systems in the past years [8, 9]. Such as many carbon materials and conductive polymers are designed as sulfur / carbon composites, sulfur / conductive polymer composites, polymer coated sulfur / carbon composites and some stable electrolytes are used to improve the electrochemical performance of Li-S batteries. However, the work about modification of separator is rarely reported. In recent years, researchers focus on the employment of coating layer on the cathode side of the separator [10-14]. For example, F. Zeng reported that the sulfonated acetylene black-coated separator which restrained polysulfide anions and improved the electronic conductivity [15]. Balach and his colleagues prepared a series of functional separators to improve the stability of Li-S batteries, including mesoporous carbon coatings [4] and N, S dual-doped mesoporous carbon coatings [16]. All of above reports show that the modification of separators has become an effective way to solve these challenges in the Li-S batteries [17, 18].

Herein, we propose a method for modifying both sides of the PP separator with super P and  $\text{Al}_2\text{O}_3$  (SGA separator). That is, super P is coated on the separator near the cathode side, while  $\text{Al}_2\text{O}_3$  is coated on the separator near the anode side. Different from the previous work of only coating the cathode side of the separator, the double side coated separator not only can improve the electronic conductivity but also inhibit the shuttle effect via physical adsorption of polysulfide.

## 2. EXPERIMENTAL

### 2.1 Preparation of (SGA) separator

First, super P (Carbon black, battery grade, made in Swiss Timcal) and Polyvinylidene fluoride (PVDF) at a weight ratio of 9 : 1 were homogeneously mixed, adding an appropriate amount of N-methyl-2-pyrrolidone (NMP) and the mixture was treated with a magnetic stirrer about 2 h to obtain a homogeneously slurry. Next, the super P slurry was uniformly coated on a PP separator (Celgard 2400) with a blade, and dried at 60 °C, the super P with a thickness of 3 ~ 5  $\mu\text{m}$ . In the same way, the other side of the PP separator was coated with  $\text{Al}_2\text{O}_3$ , and the thickness of the  $\text{Al}_2\text{O}_3$  coating was 4  $\mu\text{m}$ .

### 2.2 Cathode preparation and battery assembly

The mixture of elemental sulfur (Aladdin, AR), super P and PVDF was mixed at a mass ratio of 7 : 2 : 1 to prepare the cathode slurry. The slurry was uniformly coated on aluminum foil with a

thickness of 20  $\mu\text{m}$  and vacuum-dried at 60  $^{\circ}\text{C}$  for 24 h. Then, it was made into a cathode disc with a diameter of 15 mm. Finally, the SGA separator was coated with super P facing the cathode and assembled into a CR2016 battery in a glove box filled with argon. The anode is metal lithium (Shanghai, 99.5%), the electrolyte is 1.0 mol L<sup>-1</sup> LiTFSI / DME + DOL (volume ratio of 1 : 1) and containing 0.1 mol L<sup>-1</sup> LiNO<sub>3</sub>.

### 2.3 Materials characterization

The surface morphology of the PP separator, super P coating, and Al<sub>2</sub>O<sub>3</sub> coating was observed with an Ultra 55 Scanning Electron Microscope (Germany). Elemental distribution of cycled SGA separator was determined by energy dispersive spectroscopy (EDS). It is necessary to remove LiTFSI in the recycled separator with 1 mol L<sup>-1</sup> DME + DOL (volume ratio 1 : 1) before characterization.

### 2.4 Electrochemical measurements

The constant current charge and discharge and rate performance of batteries was tested by CT2001A battery test system (Wuhan) at room temperature. The electrochemical impedance spectroscopy (EIS) and Cyclic voltammetry (CV) tests were performed on a CHI660E electrochemical workstation (Shanghai). Cyclic voltammetry test voltage is 1.5 ~ 3.0 V, the scan rate is 0.1 mV s<sup>-1</sup>. EIS test frequency is 10<sup>-2</sup> ~ 10<sup>5</sup> Hz, the amplitude is  $\pm 5$  mV.

## 3. RESULTS AND DISCUSSION

### 3.1 Materials characterization

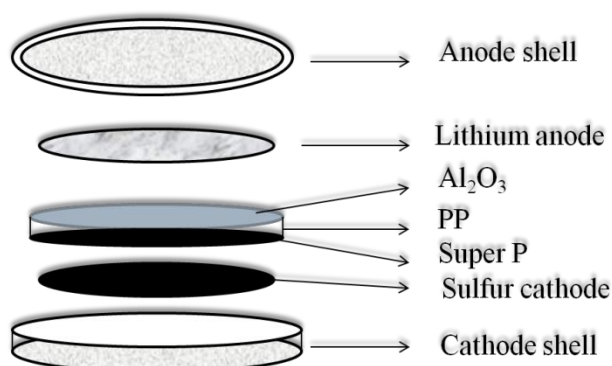


**Figure 1.** A schematic illustration of a SGA separator assembled into a battery

Fig. 1 is a schematic illustration of a SGA separator assembled into a battery. The super P layer side is towards the pure sulfur cathode, the other side of the Al<sub>2</sub>O<sub>3</sub> layer faces the metal lithium anode. In order to study the mechanism of the modified separator to suppress the shuttle effect of polysulfide,

the modified separator was analyzed by scanning electron microscopy and X-ray energy scattering analysis, as shown in Fig. 2. Fig. 2a, Fig. 2b and Fig. 2c are the SEM images of the PP layer, the super P layer and the  $\text{Al}_2\text{O}_3$  layer before the cycle. The PP separator exhibits uniform submicron pores as shown in Fig. 2a, and the polysulfide easily reaches the anode. Fig. 2b shows that the super P is coated on the PP separator and is well adhered to the separator. Fig. 2c shows that the  $\text{Al}_2\text{O}_3$  layer uniformly anchors on the separator, its role is to enhance the thermal stability of the separator [19, 20]. Fig. 2d and Fig. 2e are the SEM images of super P layer and  $\text{Al}_2\text{O}_3$  layer after 50 cycles respectively, it can be clearly seen that the basic morphologies maintain very well.

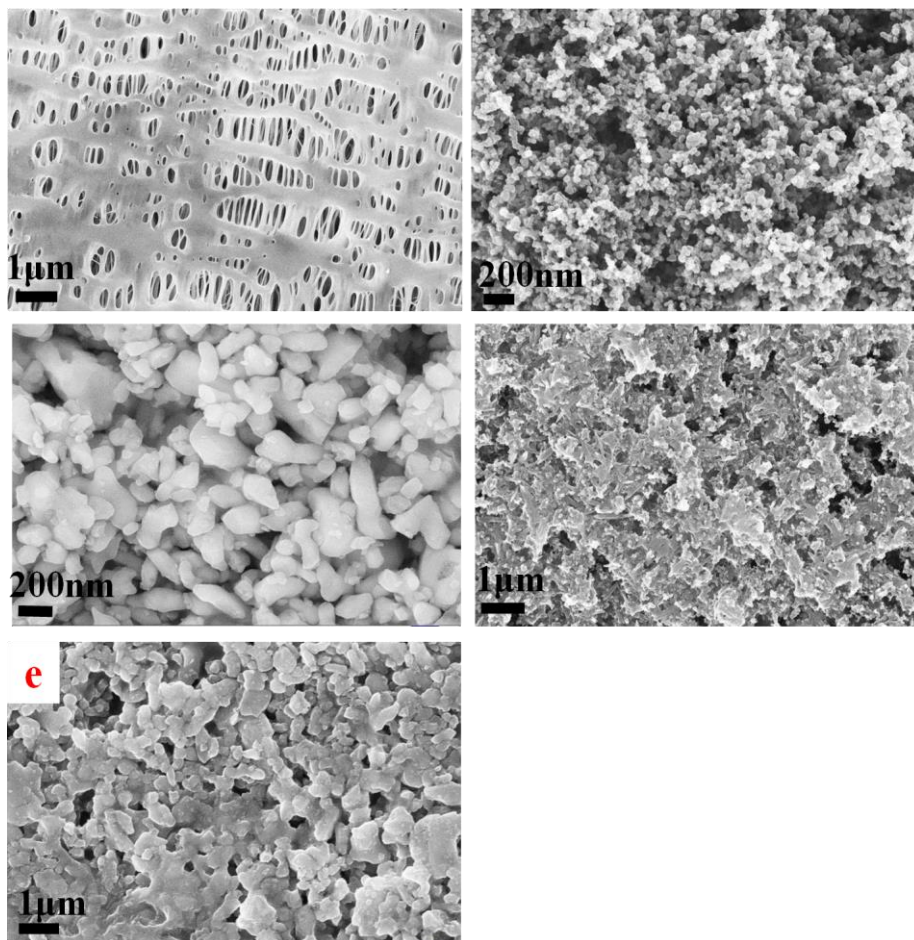


**Figure 2.** The SEM image of the modified separator (Fig. 2a is the SEM image of the PP separator and Fig. 2b, 2c, 2d, 2e are the SEM image of the super P layer and the  $\text{Al}_2\text{O}_3$  layer before the cycle and after 50 cycles, respectively)

Fig. 3a and Fig. 3b show the X-ray energy dispersive (EDS) of the super P layer and the  $\text{Al}_2\text{O}_3$  layer for the S element after 50 cycles, respectively. As shown in Fig. 3a, there are a lot of S elements on the super P layer, which indicate that super P attracts polysulfide by enhancing the absorption of electrolyte to a large extent [21, 22]. Fig. 3b shows that the presence of trace elements in the  $\text{Al}_2\text{O}_3$  layer. It illustrate that there is still microscale polysulfides passed through the PP separator but they are fixed in the  $\text{Al}_2\text{O}_3$  layer, which avoids the deposition on the surface of lithium metal. That is, the  $\text{Al}_2\text{O}_3$

layer also has a certain adsorption effect for the polysulfide and it is another barrier to prevent polysulfide diffusion to anode.

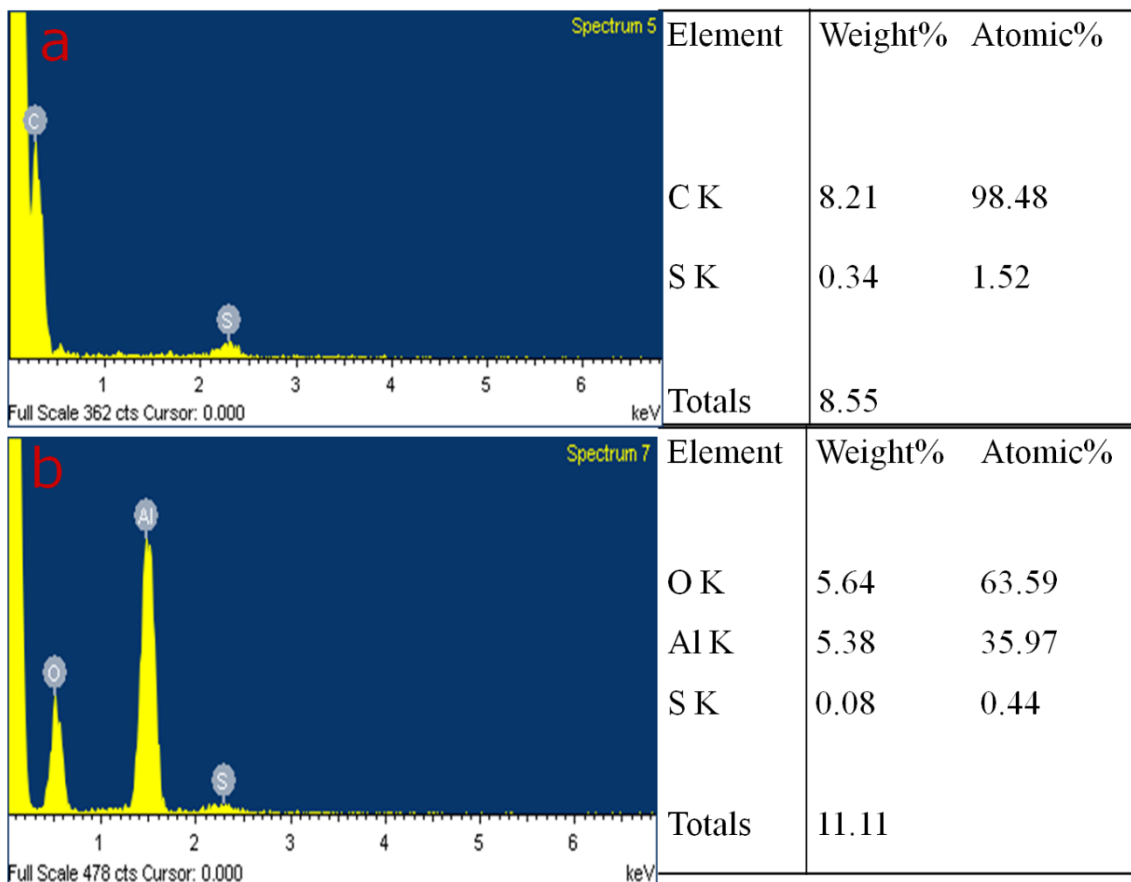


**Figure 3.** The EDS image of the separators after 50 cycles (Fig. 3a, 3b are the energy dispersive X-ray images of the super P layer and the Al<sub>2</sub>O<sub>3</sub> layer for the S element after 50 cycles, respectively)

### 3.2 Electrochemical Analysis

In order to study the effect of the modified separator on the electrochemical performance of the batteries, we assembled a series of different types of lithium-sulfur button batteries, including SGA separator, SP + PP separator (SG separator, SP layer faced the cathode), PP + Al<sub>2</sub>O<sub>3</sub> separator (GA separator, the Al<sub>2</sub>O<sub>3</sub> layer faced the anode) and PP separator (unmodified).

Fig. 4a shows the initial charge / discharge curve of the batteries with four different separators at 0.1 C. The first discharge capacity of the batteries assembled with SGA separators, SG separators, GA separators, PP separators is 1247 mAh g<sup>-1</sup>, 806.9 mAh g<sup>-1</sup>, 721.5 mAh g<sup>-1</sup>, 670.1 mAh g<sup>-1</sup>. Compared with the battery with unmodified PP separator, the initial discharge capacity of the modified batteries is improved more or less. Especially, the specific discharge capacity of SGA separator is most obvious to improve. Fig. 4b shows the cyclic voltammetry (CV) of the batteries at 0.1 mV s<sup>-1</sup> scanning speed. Two reduction peaks appeared in the Fig. 4b and the reduction peak appeared at 2.3 V corresponding to the conversion of elemental sulfur into highly-polymerized polysulfides (soluble), the reduction peak appearing at 2.0 V corresponded to the high polysulfide into the oligomeric

polysulfides (insoluble). Only oxidation peak at 2.5 V conversion of lithium sulfide into oxidized active S ( $\text{Li}_2\text{S}_8$  or S) [23]. The batteries with modified separators as a whole show a tendency that the oxidation peaks are shifted to the left and the reduction peaks are shifted right. The oxidation-reduction potential difference becomes smaller, the battery polarization becomes smaller and the reversibility becomes better.

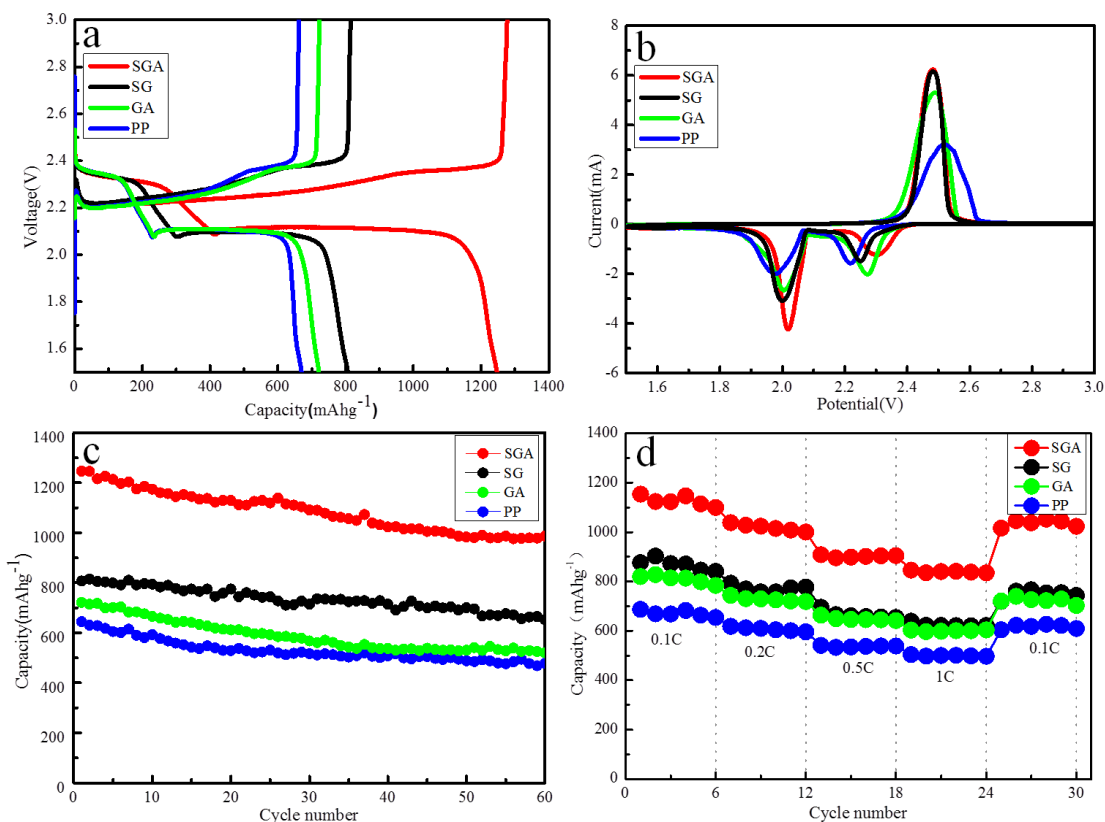


**Figure 4.** (a) the initial charge / discharge curve at 0.1 C. (b) the CV curves. (test voltage is 1.5 ~ 3.0 V, the scan rate is  $0.1 \text{ mV s}^{-1}$ ) (c) the cycle performance at 0.1 C. (d) the rate performance at 0.1 C, 0.2 C, 0.5 C, 1 C, 0.1 C.

This indicates that the modified separator can suppress polysulfide to cross the separator to some extent, resulting in irreversible loss of capacity. Moreover, it can be observed that the battery with SGA separator has the largest reduction peak intensity and the corresponding discharge capacity is the largest. The result is consistent with the result of the initial charge / discharge. Fig. 4c shows the cycling performance of different separators in the Li-S battery at the current density of 0.1 C. After 60 cycles, the discharge capacity of the battery with SGA separator is still  $987 \text{ mAh g}^{-1}$  and the capacity retention ratio is 79%, exhibiting excellent cycle stability. In contrast, the battery assembled with an unmodified PP separator shows poorer cycle performance due to the diffusion of large amounts of polysulfides to the anode. Fig. 4d exhibits the rate performance of four batteries at 0.1 C, 0.2 C, 0.5 C, 1 C, 0.1 C current density. As can be seen from the Fig. 4d the battery with SGA separator is the best

rate performance. When the current suddenly changes from 1 C to 0.1 C, the discharge capacity can be returned to 92% of the initial capacity at 0.1 C.

In order to clarify the reason which the Li-S batteries assembled with the modified separator have more excellent electrical properties, the AC impedance measurement of Li-S batteries with SGA separator, SG separator, GA separator and PP separator is carried out. As shown in Fig. 5, The semicircle in the high frequency region and the slash in the low frequency region make up the Nyquist plot. The semicircle of the high frequency region represents the charge transfer resistance in the electrolyte and the electrode ( $R_{ct}$ ), the intercept of the oblique line at the real axis represents the intrinsic resistance of the active materials and the interfacial impedance of the electrolyte and the electrode ( $R_e$ ) [24]. The batteries with SG separator and SGA separator have the smallest semicircle, indicating that the charge transfer resistance is least. The result of fitting through the equivalent circuit is shown in Table 1. It can also be seen that the SGA separator has the smallest values of  $R_{ct}$  and has the smallest charge transfer resistance. This is due to the reason that the super P has excellent electrical conductivity, which facilitates fast ionic transport and reduce the charge transfer resistance in the electrode.

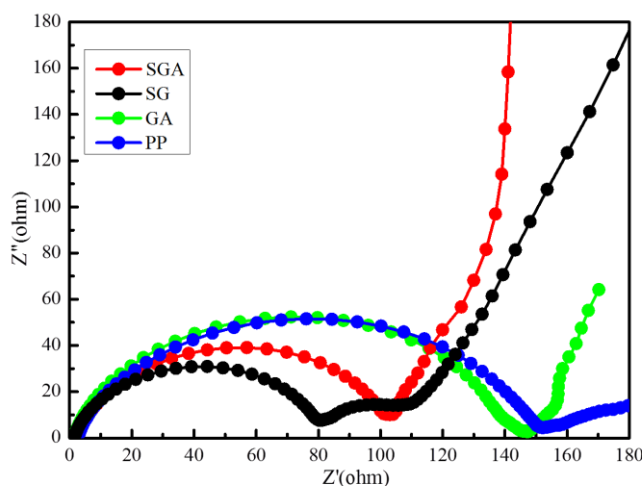


**Figure 5.** EIS spectra of Li-S batteries with PP, SGA, SG and GA separators (test frequency is  $10^{-2} \sim 10^5$  Hz, the amplitude is  $\pm 5$  mV)

**Table 1.** The impedance parameters of Li-S batteries with PP, SGA, SG and GA separators

separator	$R_e(\Omega)$	$R_{ct}(\Omega)$
SGA	2.35	100.65
SG	1.88	103.82
GA	1.97	145.53
PP	3.21	148.89

#### 4. CONCLUSIONS

The experimental results show that the batteries assembled with the SGA separator exhibit optimal electrochemical performance. The initial discharge capacity is 1247 mAh g<sup>-1</sup> at the current density of 0.1 C. The discharge capacity is still 987 mAh g<sup>-1</sup> after 60 cycles. The reason for the improvement of electrochemical performance is that the super P layer has excellent electrical conductivity which facilitates fast ionic transport, while the super P can adsorb polysulfide and inhibit the shuttle effect, the Al<sub>2</sub>O<sub>3</sub> layer can improve the mechanical properties of the separator which is also another barrier to resist the polysulfide diffusion to the anode. In summary, the SGA separator provides a guideline for the production of high energy lithium-sulfur batteries.

#### ACKNOWLEDGEMENTS

This work was financially supported by the LongShan academic talent research supporting program of SWUST (17LZX507).

#### References

1. X. Ji and L.F. Nazar, *J. Mater. Chem.*, 20 (2010) 9821.
2. A. Manthiram, Y. Fu and Y.S. Su, *Acc. Chem. Res.*, 46 (2013) 1125.
3. P.G. Bruce, S.A. Freunberger, L.J. Hardwick and J.M. Tarascon, *Nat. Mater.*, 11 (2012) 19.
4. J. Balach, T. Jaumann, M. Klose, S. Oswald, J. Eckert and L. Giebeler, *Adv. Funct. Mater.*, 25 (2015) 5285.
5. Y.V. Mikhaylik and J.R. Akridge, *J. Electrochem. Soc.*, 151 (2004) A1969.
6. Y. Qiu, W. Li, W. Zhao, G. Li, Y. Hou, M. Liu, L. Zhou, F. Ye, H. Li and Z. Wei, *Nano lett.*, 8 (2014) 4821.
7. H. Wang, Y. Yang, Y. Liang, J.T. Robinson, Y. Li, A. Jackson, Y. Cui and H. Dai, *J. Am. Chem. Soc.*, 132 (2010) 13978.
8. M.U. Patel, R. Demir-Cakan, M. Morcrette, J. Tarascon, M. Gaberscek and R. Dominko, *Chemsuschem*, 6 (2013) 1177.
9. Y. Yang, G. Zheng and Y. Cui, *Energy Environ. Sci.*, 6 (2013) 1552.
10. S. Zhu, Y. Wang, J. Jiang, X. Yan and D. Sun, *ACS Appl. Mater. Interfaces*, 8 (2016) 17253.
11. H. Wang, W. Zhang, H. Liu and Z. Guo, *Angew. Chem. Int. Ed.*, 55 (2016) 3992.
12. T.Z. Zhuang, J.Q. Huang, H.J. Peng, L.Y. He and X.B. Cheng, *Small*, 12 (2016) 381.
13. C.H. Chang, S.H. Chung and A. Manthiram, *J. Mater. Chem.*, 3 (2015) 18829.
14. U. Stoeck, J. Balach, M. Klose, D. Wadewitz and E. Ahrens, *J. Power Sources*, 309 (2016) 76.
15. F. Zeng, Z. Jin, K. Yuan, S. Liu and X. Cheng, *J. Mater. Chem.*, 4 (2016) 12319.
16. J. Balach, H.K. Singh, S. Gomoll, T. Jaumann and M. Klose, *ACS Appl. Mater. Interfaces*, 8 (2016) 14586.
17. X. Gu, C.J. Tong, C. Lai, J. Qiu and X. Huang, *J. Mater. Chem.*, 3 (2015) 9502.
18. H. Wei, J. Ma, B. Li, Y. Zuo and D. Xia, *ACS Appl. Mater. Interfaces*, 6 (2014) 20276.
19. H.W. Kwak, Y. Kim, N.K. Yun and K.H. Lee, *Macromol. Res.*, 22 (2014) 788.
20. R. Song, R. Fang, L. Wen, Y. Shi and S. Wang, *J. Power Sources*, 301 (2016) 179.
21. S.H. Chung and A. Manthiram, *Adv. Funct. Mater.*, 24 (2014) 5299.
22. H. Yao, K. Yan, W. Li, G. Zheng, D. Kong, Z.W. Seh, V.K. Narasimhan, Z. Liang and Y. Cui, *Energy Environ. Sci.*, 7 (2014) 3381.
23. Y.S. Su and A. Manthiram, *Electrochim. Acta*, 77 (2012) 272.

24. H. Lu, Y. Yuan, Z. Hou, Y. Lai and K. Zhang, *RSC Adv.*, 6 (2016) 18186.

© 2018 The Authors. Published by ESG ([www.electrochemsci.org](http://www.electrochemsci.org)). This article is an open access article distributed under the terms and conditions of the Creative Commons Attribution license (<http://creativecommons.org/licenses/by/4.0/>).